J|A|C|S ARTICLES

Published on Web 12/13/2010

Influence of Excitation Wavelength (UV or Visible Light) on the Photocatalytic Activity of Titania Containing Gold Nanoparticles for the Generation of Hydrogen or Oxygen from Water

Cláudia Gomes Silva,[†] Raquel Juárez,[†] Tiziana Marino,[†,‡] Raffaele Molinari,[‡] and Hermenegildo García*[,†]

Instituto Universitario de Tecnología Química (CSIC-UPV), Universidad Politecnica de Valencia, Av. de los Naranjos s/n, 46022, Valencia, Spain, and Department of Chemical and Materials Engineering, University of Calabria, Via P. Bucci, 44/A, I-87036 Rende, CS, Italy

Received September 24, 2010; E-mail: hgarcia@qim.upv.es

Abstract: Gold nanoparticles supported on P25 titania (Au/TiO_2) exhibit photocatalytic activity for UV and visible light (532 nm laser or polychromatic light $\lambda > 400$ nm) water splitting. The efficiency and operating mechanism are different depending on whether excitation occurs on the titania semiconductor (gold acting as electron buffer and site for gas generation) or on the surface plasmon band of gold (photoinjection of electrons from gold onto the titania conduction band and less oxidizing electron hole potential of about −1.14 V). For the novel visible light photoactivity of Au/TiO_2, it has been determined that gold loading, particle size and calcination temperature play a role in the photocatalytic activity, the most active material ($\Phi_{H2} = 7.5\%$ and $\Phi_{O2} = 5.0\%$ at 560 nm) being the catalyst containing 0.2 wt % gold with 1.87 nm average particle size and calcined at 200 °C.

Introduction

Titanium dioxide is the most widely used photocatalyst.[1−5] In spite of the advantages of TiO_2 in terms of availability, low toxicity and robustness under operation conditions, TiO_2 is far from being a perfect photocatalyst, there being still room for efficiency improvement in most photocatalytic processes using UV light and also to introduce visible light photoactivity in TiO_2. Doping with metals, particularly noble, nonmetallic elements, such as N, C and S, encapsulation of I_2 or organic dye sensitization has been widely used to overcome the lack of visible light response of TiO_2.[6−11] In this regard, one alternative that is attracting increasing interest to effect the photosensitization of titania is the use of gold nanoparticles deposited on the titania surface (Au/TiO_2).[12−16] Gold is a noble metal that does not undergo corrosion under photocatalytic conditions, it can be prepared strongly anchored on the titania surface and it exhibits a characteristic surface plasmon band in the visible region due to the collective excitation of electrons in the gold nanoparticles.[17,18] Part of the interest of employing Au/TiO_2 in photocatalysis arises from the use of this material as heterogeneous catalyst.

In contrast to the numerous reports dealing with the photocatalytic activity of doped and undoped TiO_2 as well as the thermal catalytic activity of Au/TiO_2, the number of reports dealing with the photocatalytic activity of Au/TiO_2 is still very scarce, and it is of interest to expand the use of Au/TiO_2 as photocatalyst.[19−22]

[†] Universidad Politecnica de Valencia.
[‡] University of Calabria.

(1) Carp, O.; Huisman, C. L.; Reller, A. *Prog. Solid State Chem.* **2004**, *32*, 33–177.
(2) Hoffmann, M. R.; Martin, S. T.; Choi, W.; Bahnemann, D. *Chem. Rev.* **1995**, *95*, 69–96.
(3) Legrini, O.; Oliveros, E.; Braun, A. M. *Chem. Rev.* **1993**, *93*, 671–698.
(4) Mills, A.; LeHunte, S. *J. Photochem. Photobiol., A* **1997**, *108*, 1–35.
(5) Pellizetti, E.; Minero, C. *Electrochim. Acta* **1993**, *38*, 47–55.
(6) Asahi, R.; Morikawa, T.; Ohwaki, T.; Aoki, K.; Taga, Y. *Science* **2001**, *293*, 269–271.
(7) Choi, W. Y.; Termin, A.; Hoffmann, M. R. *J. Phys. Chem.* **1994**, *98*, 13669–13679.
(8) Gratzel, M. *Inorg. Chem.* **2005**, *44*, 6841–6851.
(9) Livraghi, S.; Paganini, M. C.; Giamello, E.; Selloni, A.; Di Valentin, C.; Pacchioni, G. *J. Am. Chem. Soc.* **2006**, *128*, 15666–15671.
(10) Ma, T. L.; Akiyama, M.; Abe, E.; Imai, I. *Nano Lett.* **2005**, *5*, 2543–2547.
(11) Usseglio, S.; Damin, A.; Scarano, D.; Bordiga, S.; Zecchina, A.; Lamberti, C. *J. Am. Chem. Soc.* **2007**, *129*, 2822–2828.
(12) Kowalska, E.; Abe, R.; Ohtani, B. *Chem. Commun.* **2009**, 241–243.
(13) Rodriguez-Gonzalez, V.; Zanellac, R.; del Angela, G.; Gomeza, R. *J. Mol. Catal. A: Chem.* **2008**, *281*, 93–98.
(14) Subramanian, V.; Roeder, R. K.; Wolf, E. E. *Ind. Eng. Chem. Res.* **2006**, *45*, 2187–2193.
(15) Zang, L.; Macyk, W.; Lange, C.; Maier, W. F.; Antonius, C.; Meissner, D.; Kisch, H. *Chem.—Eur. J.* **2000**, *6*, 379–384.
(16) Primo, A.; Corma, A.; Garcia, H. *Phys. Chem. Chem. Phys.* DOI: 10.1039/C0CP00917B.
(17) El-Brolossy, T. A.; Abdallah, T.; Mohamed, M. B.; Abdallah, S.; Easawi, K.; Negm, S.; Talaat, H. *Eur. Phys. J.—Spec. Top.* **2008**, *153*, 361–364.
(18) Orendorff, C. J.; Sau, T. K.; Murphy, C. J. *Small* **2006**, *2*, 636–639.
(19) Arabatzis, I. M.; Stergiopoulos, T.; Andreeva, D.; Kitova, S.; Neophytides, S. G.; Falaras, P. *J. Catal.* **2003**, *220*, 127–135.
(20) Carneiro, J. T.; Yang, C. C.; Moma, J. A.; Moulijn, J. A.; Mul, G. *Catal. Lett.* **2009**, *129*, 12–19.
(21) Ismail, A. A.; Bahnemann, D. W. *J. Adv. Oxid. Technol.* **2009**, *12*, 9–15.
(22) Ismail, A. A.; Bahnemann, D. W.; Bannat, I.; Wark, M. *J. Phys. Chem. C* **2009**, *113*, 7429–7435.

Besides degradation of organic pollutants (*environmental photocatalysis*),[23−28] one potentially important application of photocatalysis is the conversion of light into chemical energy.[29−33] In this regard photocatalytic water splitting is a challenging process due to the low efficiency of the systems that have been reported.[34]

In the present work we describe that Au/TiO_2 exhibits for photocatalytic water splitting two distinctive operating mechanisms depending on the excitation (UV or visible light) wavelength. Importantly, evidence will be presented firmly supporting the operation of visible light water splitting arising from the excitation of the gold surface plasmon. We will show that the visible light photocatalytic activity of Au/TiO_2 depends on the particle size and the preparation procedure. While there are some reports in the literature describing the use of Au/TiO_2 as photocatalyst, even using visible light illumination,[16] none of them have dealt with visible light photocatalytic water splitting.

In a related precedent, Haruta studied the photocatalytic activity for water splitting upon UV excitation of some gold catalysts compared with platinum.[35] It was observed that the activity of gold samples was about 30% lower than that of platinum. In addition, they observed that the activity of titania supported gold was very sensitive to the preparation procedure.[35] But the experimental results were explained just considering Au nanoparticles as catalytic centers for gas generation without being responsible for light absorption.

Recently, Wark and co-workers have reported the use of Au/TiO_2 to enhance the photocatalytic activity of TiO_2 for methanol oxidation to formaldehyde irradiating at wavelengths longer than 320 nm.[22] In other cases, it has been observed that the presence of Au nanoparticles is even detrimental for the inherent photocatalytic activity of TiO_2. For instance, Mul and co-workers have checked Au/TiO_2 to promote the aerobic oxyfunctionalization of cyclohexane to mixtures of cyclohexanol/cyclohexanone and found that Au nanoparticles decrease the photocatalytic activity due to the reduction of the surface OH population required in the photocatalytic process.[20] Thus, the present situation does not allow concluding the positive or negative effect of gold nanoparticles on the photocatalytic activity of titania.[20] As we have indicated, these prior studies were performed using light in the UV range, and therefore exciting directly the TiO_2 semiconductor absorption band. The possibility of using the surface plasmon band of gold nanoparticles (from 500 to 600 nm) to excite photochemically the Au/TiO_2 system has been up to now mostly neglected. Only a few scattered precedents have reported visible light photoactivity of Au/TiO_2 such as in the degradation of chemical warfare agents.[36]

In the present work we will show also the visible light photocatalytic activity of Au/TiO_2. The main difference with the previous work is that gold nanoparticles exhibit a dual role as light harvesters injecting electrons into the semiconductor conduction band and also as catalytic sites for gas generation. Besides the photocatalytic activity for hydrogen generation using sacrificial electron donors, we have also determined the activity of Au/TiO_2 for the visible light oxygen formation adding sacrificial electron acceptors. Considering the interest in gold catalysis, our finding can open new avenues aimed at applying this type of catalyst into photocatalysis.

Experimental Section

Photocatalyst Synthesis. Au(1.5 wt %)/TiO_2 consists of 1.5 wt % gold on P25 TiO_2 and was supplied by Gold World Council (reference catalyst Type A). Materials containing different gold percentages were prepared by depositing the gold from an aqueous solution of $HAuCl_4$ (Alfa Aesar) on a sample of TiO_2 (P25 Degussa). The deposition precipitation procedure is done at 343 K and pH 9 during 2 h, using (0.2 M) NaOH to maintain the pH constant. Under these conditions, gold deposition occurs with 80% efficiency. The catalyst is then recovered, filtered, washed with deionized water, and dried at 373 K overnight. Finally, the powder is calcined at 673 K in air for 4 h.[37,38] Particles of different sizes were obtained by changing the pH used in the deposition of gold nanoparticles over the TiO_2 support and the calcination temperature. Thus, a solution of $HAuCl_4 \cdot 3H_2O$ (50 mg) in 100 mL of Milli-Q water was brought to pH 4.5, 6.0, or 9.0 by addition of a 0.2 M solution of NaOH. Once the pH value was stable 300 mg of P25 TiO_2 was added. The slurry was vigorously stirred overnight. The Au/TiO_2 catalyst was then filtered and exhaustively washed with Milli-Q water. The catalyst was dried at 100 °C during 8 h and calcined at 200 or 400 °C. The temperature program starts at room temperature increasing at a rate of 5 °C min^{-1} up to the final temperature that was maintained for 4 h.

Material Characterization. Room temperature diffuse reflectance UV−vis−NIR spectra of solid samples were recorded by the diffuse reflectance mode using an integrating sphere with a Varian Cary 5000 UV−vis−NIR scanning spectrophotometer. The gold content of the catalysts was determined using an inductively coupled plasma optical emission spectrometer (ICP-OES, Varian). TEM images were obtained using a Jeol 200 Cx microscope operating at 200 kV.

The interaction of gold nanoparticles with titania support was addressed by XP spectroscopy, monitoring the Au $4f_{7/2}$ peak of gold. The experimental XPS peaks indicate the presence of Au(0) with binding energies of 87.4 and 83.7 eV that are somewhat shifted toward lower energy than binding energies of metallic Au.[39] This indicates a charge transfer from the P25 TiO_2 support to the gold nanoparticles.

Photocatalytic Tests. The photocatalytic experiments were carried out in a 30 mL Pyrex reactor. The headspace of the reactor was connected to an inverted buret filled with water at atmospheric

(23) Bayarri, B.; Carbonell, E.; Gimenez, J.; Esplugas, S.; Garcia, H. *Chemosphere* **2008**, *72*, 67–74.
(24) da Silva, C. G.; Faria, J. L. *J. Photochem. Photobiol., A* **2003**, *155*, 133–143.
(25) Navalon, S.; Alvaro, M.; Garcia, H.; Escrig, D.; Costa, V. *Water Sci. Technol.* **2009**, *59*, 639–645.
(26) Silva, A. M. T.; Silva, C. G.; Drazic, G.; Faria, J. L. *Catal. Today* **2009**, *144*, 13–18.
(27) Silva, C. G.; Wang, W. D.; Faria, J. L. *J. Photochem. Photobiol., A* **2006**, *181*, 314–324.
(28) Hoffmann, M. R.; Martin, S. T.; Choi, W. Y.; Bahnemann, D. W. *Chem. Rev.* **1995**, *95*, 69–96.
(29) Atienzar, P.; Navarro, M.; Corma, A.; Garcia, H. *ChemPhysChem* **2009**, *10*, 252–256.
(30) Gratzel, M. *Nature* **2001**, *414*, 338–344.
(31) Matsuoka, M.; Kitano, M.; Takeuchi, M.; Tsujimaru, K.; Anpo, M.; Thomas, J. M. *Catal. Today* **2007**, *122*, 51–61.
(32) Silva, C. G.; Bouizi, Y.; Fornes, V.; Garcia, H. *J. Am. Chem. Soc.* **2009**, *131*, 13833–13839.
(33) Teruel, L.; Alonso, M.; Quintana, M. C.; Salvador, A.; Juanes, O.; Rodriguez-Ubis, J. C.; Brunet, E.; Garcia, H. *Phys. Chem. Chem. Phys.* **2009**, *11*, 2922–2927.
(34) Yerga, R. M. N.; Galvan, M. C. A.; del Valle, F.; de la Mano, J. A. V.; Fierro, J. L. G. *ChemSusChem* **2009**, *2*, 471–485.
(35) Bamwenda, G. R.; Tsubota, S.; Nakamura, T.; Haruta, M. *J. Photochem. Photobiol., A* **1995**, *89*, 177–189.
(36) Neatu, S.; Cojocaru, B.; Parvulescu, V. I.; Somoghi, V.; Alvaro, M.; Garcia, H. *J. Mater. Chem.* **2010**, *20*, 4050–4054.
(37) Grirrane, A.; Corma, A.; Garcia, H. *Nat. Protoc.* **2010**, *5*, 429–438.
(38) Grirrane, A.; Corma, A.; Garcia, H. *Science* **2008**, *322*, 1661–1664.
(39) Zwijnenburg, A.; Goossens, A.; Sloof, W. G.; Craje, M. W. J.; van der Kraan, A. M.; de Jongh, L. J.; Makkee, M.; Moulijn, J. A. *J. Phys. Chem. B* **2002**, *106*, 9853–9862.

pressure, allowing the measurement of the evolved gas. In the photocatalytic reactions for hydrogen generation, Au/TiO_2 powders (45 mg) were dispersed in water/methanol solutions (H_2O:methanol of 3:1 v/v %) or water containing 0.02 M of EDTA. In the case of the photocatalytic oxygen generation reactions, the same amount of catalyst was dispersed in a 0.01 M $AgNO_3$ aqueous solution in the reaction cell. In both cases, the total volume of the suspensions was of 22.5 mL. The suspensions were purged with an argon flow for at least 30 min before irradiation in order to remove dissolved air. Then the suspensions were irradiated for 3 h using either a 200 W xenon-doped mercury lamp (Hamamatsu Lightningcure LC8, 1 cm distance) or the second harmonic of a Nd:YAG laser (532 nm, 7 ns pulse width, ≥ 50 mJ $\times$ pulse^{-1}). For polychromatic visible light irradiation the output of the 220 W xenon-doped mercury lamp was filtered through a cutoff filter ($\lambda > 400$ nm). The stationary temperature of the reactor, reached at 5 min of irradiation, was lower than 38 °C. The formation of hydrogen and oxygen was confirmed by injecting 0.5 mL of the reactor headspace gas in a gas chromatograph (HP 5890) operating at isothermal conditions (50 °C) using a semicapillary column (molecular sieve, 530 μm diameter, 15 m length) equipped with a thermal conductivity detector and argon as carrier gas.

Electrochemical Characterization. Electrochemical measurements were carried out using the conventional three electrode setup connected to an Amel potentiostat (model 7050) that was controlled by software allowing data storage and management. As working electrode a thin film of Au/TiO_2 was deposited using the doctor blade technique on a FTO conductive support. A paste of methylcellulose and terpineol in acetone containing about 30% Au/TiO_2 in weight was prepared by mechanical mixing and then spread on the FTO electrode. Before measurements the paste was dried at room temperature and then calcined at 400 °C heating from room temperature at 5 °C min^{-1} and maintaining the maximum temperature for 1 h. As counter and reference electrodes a platinum wire and a 0.1 M Ag/AgCl standard solution were used, respectively. The FTO electrode containing the Au/TiO_2 film and the counter electrode were immersed into 0.1 M tetrabutylammonium perchlorate electrolyte in acetonitrile. Measurements were carried out at a scan rate of 50 mV s^{-1} in the range $-2.0/+2$ V.

Apparent Quantum Yield Measurements. Photon flux was determined using a 150 W mercury lamp at 560 nm using a monochromator (half-width 12 nm) by potassium ferrioxalate actinometry being of 4.38 Einstein s^{-1}. The actinometer solution was irradiated for 2 min using monochromatic light. The number of photons entering the reaction system is determined by measuring Fe^{2+} formation via the visible absorption spectroscopy of Fe^{2+}−phenanthroline complex at 510 nm, knowing that, at the working conditions, this photocomplexation reaction has a quantum yield of 1.21.[40] Then, photocatalytic hydrogen or oxygen generation reactions were performed using monochromatic light. After 3 h of irradiation the amount of gas evolved was determined by gas chromatography. The quantum yield of the photocatalytic reactions was determined by the ratio between the number of reacted electrons/holes that are related to the number of hydrogen/oxygen molecules formed, and the number of incident photons.

Results and Discussion

Preliminary tests by irradiating suspensions of Au/TiO_2 in water/methanol solution for several days and analysis of the gold leaching in the solution demonstrated the stability of the Au/TiO_2 upon exposure to the light and the possibility to use it as photocatalyst. The overall water splitting consists of the combination of the reduction to hydrogen and oxidation to oxygen semireactions. In order to gain understanding on the rate-determining process that eventually can lead to more efficient photocatalysts it is very convenient to study both semireactions separately. This can be carried out by adding sacrificial electron donors when studying the reduction process and sacrificial electron acceptors when performing the oxidation semireaction.[41] In the present study we started addressing the photocatalytic hydrogen formation with either UV or visible light in the presence of a series of gold nanoparticles supported on P25 titania (Au/TiO_2) photocatalysts using methanol or EDTA as sacrificial reducing agents. P25 is considered a reference for titania photocatalysts, and typically the photocatalytic activity of any new material is contrasted with that of P25 standard.[42,43] P25, although it consists predominantly of the anatase phase, contains also about 20% of rutile, the combination of both phases being optimal for many photocatalytic reactions.[44,45] It remains to be seen what would be the photocatalytic activity of gold supported on pure anatase or rutile phases.

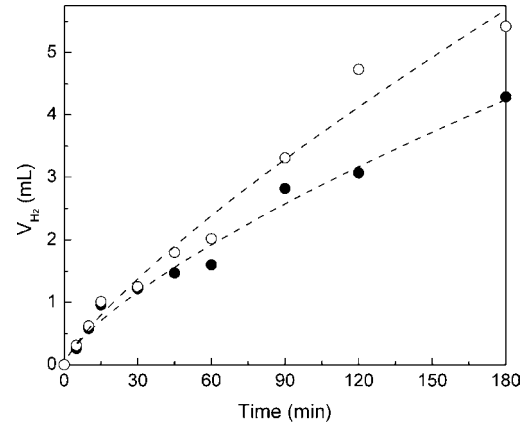

Figure 1. Influence of pH on the volume of hydrogen evolved (V_{H2}) during the photocatalytic runs using Au(1.5 wt %)/TiO_2 catalyst and EDTA as sacrificial electron donor at two different initial pH values. ○: pH 7.00. ●: pH 2.65.

UV Light Photocatalytic Hydrogen Generation. In the first stage of our work we checked the ability of Au(1.5 wt %)/TiO_2 to generate hydrogen upon irradiation with a Xe-doped Hg lamp of water containing EDTA as sacrificial electron donor at two different pH values. The results are presented in Figure 1. The reproducibility of the temporal profiles and the initial reaction rates was checked by performing independent runs under identical conditions, whereby similar profiles to those shown in Figure 1 were obtained.

In this case, following the previous studies the most reasonable rationalization is indicated in Scheme 1 and assumes direct photoexcitation of TiO_2 with photons with energy larger than the bandgap ($\lambda < 380$ nm) leading to the generation of electrons in the semiconductor conduction band and electron holes in the valence band. The electron in the conduction band will move to the gold nanoparticles acting as electron buffer and catalytic sites for hydrogen generation. The electron holes will be quenched by EDTA. The influence of the pH in the photocatalytic activity is compatible with this interpretation since at higher

(40) Murov, S. L.; Carmichael, I.; Hug, G. L. *Handbook of Photochemistry*2nd ed.; Marcel Dekker: New York, 1993.
(41) Kamata, K.; Maeda, K.; Lu, D. L.; Kako, Y.; Domen, K. *Chem. Phys. Lett.* **2009**, *470*, 90–94.
(42) Maschmayer, T.; Che, M. *Angew. Chem.* **2010**, *49*, 1536–1539.
(43) Sclafani, A.; Herrmann, J. M. *J. Phys. Chem.* **1996**, *100*, 13655–13661.
(44) Ding, Z.; Lu, G. Q.; Greenfield, P. F. *J. Phys. Chem. B* **2000**, *104*, 4815–4820.
(45) Hurum, D. C.; Agrios, A. G.; Gray, K. A.; Rajh, T.; Thurnauer, M. C. *J. Phys. Chem. B* **2003**, *107*, 4545–4549.

Scheme 1. Proposed Rationalization of the Photocatalytic Activity of Au/TiO_2 under UV Light Excitation

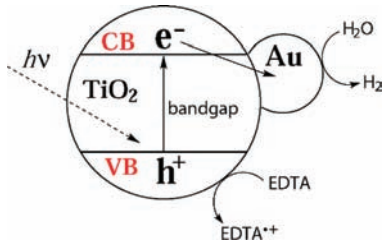

pH EDTA will be unprotonated and more prone to give electrons to the titania valence band holes.

Visible Light Photocatalytic Hydrogen Generation. In order to firmly prove the visible light photocatalytic activity of Au(1.5 wt %)/TiO_2 for hydrogen generation upon irradiation of aqueous solutions containing EDTA, the second harmonic of a Nd:YAG laser operating at 532 nm was used. Gold nanoparticles supported in titania exhibit a surface plasmon band with λ_{max} at about 550 nm, very close to the excitation wavelength used in this experiments. Figure 2 shows a comparison of the hydrogen evolved upon 532 nm laser irradiation of Au(1.5 wt %)/TiO_2 and TiO_2. As it can be seen there, the control shows that as expected TiO_2 is devoid of any photocatalytic activity under these conditions.

Figure 2 also shows the temporal hydrogen evolution using a filtered polychromatic light as excitation for Au/TiO_2. The results obtained using monochromatic laser excitation were consistent with the photocatalytic hydrogen generation using polychromatic lamp light of wavelength longer than 400 nm.

We notice that the hydrogen evolution using monochromatic 532 nm laser pulses exhibits an increase in the formation rate that could be due to several reasons, including (i) initial hydrogen absorption on the solid, (ii) changes in the gold particle size caused by the laser energy producing growth or agglomeration of gold nanoparticles, and (iii) titania phase change from anatase to rutile due to the local heat effect generated by the laser pulse. It should be noted, however, that thermal water splitting is very unlikely to be responsible for the observed hydrogen evolution since it requires temperatures well above 1000 °C.

The most reasonable mechanism for the photocatalytic hydrogen generation is depicted in Scheme 2. As it can be seen

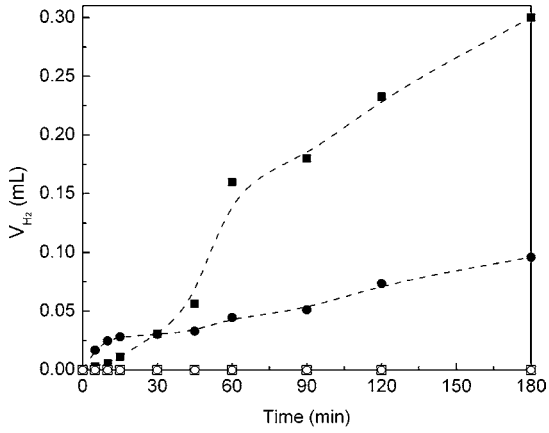

Figure 2. Volume of hydrogen evolved at atmospheric pressure and 30 °C (V_{H2}) during the photocatalytic runs using TiO_2 and Au(1.5 wt %)/TiO_2 as catalysts and EDTA as sacrificial electron donor, under 532 nm laser irradiation and polychromatic light $\lambda > 400$ nm. ■: Au/TiO_2, $\lambda = 532$ nm. ●: Au/TiO_2, $\lambda > 400$ nm. ○: TiO_2, $\lambda = 532$ nm. □: TiO_2, $\lambda > 400$ nm.

Scheme 2. Proposed Rationalization of the Photocatalytic Activity of Au/TiO_2 upon Excitation of the Gold Surface Plasmon Band

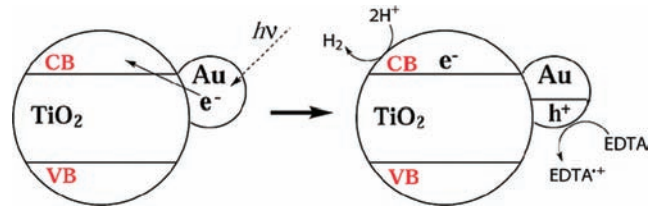

there, upon photoexcitation of Au nanoparticles, electrons from Au are injected into the TiO_2 conduction band leading to the generation of holes in the Au nanoparticles and electrons in the TiO_2 conduction band. The latter are known to effect hydrogen generation, and the holes will be quenched by EDTA as sacrificial electron donor.

Evidence in support of the proposed mechanism is the fact that the photocatalytic response for hydrogen generation agrees with the absorption of the gold surface plasmon band (see Figure 5). Moreover, controls in where colloidal solutions of gold nanoparticles stabilized with citrate were submitted to irradiation under the same conditions did not lead to observation of hydrogen evolution.

Obviously the mechanism of photochemical process indicated in Scheme 2 is an oversimplification since it has been determined that, due to the gold/titania interfacial contact, the conduction band of the semiconductor undergoes shift toward more negative potentials, the energy level being bent at the interface of titania by the influence of gold. Thus, the charge distribution between the gold nanoparticles and the semiconductor causes a shift of the Fermi level toward more negative potentials.[46,47]

The photogeneration of hydrogen using Au/TiO_2 as photocatalyst was also performed using visible light (cutoff filter, $\lambda > 400$ nm) from a Hg−Xe lamp and methanol as sacrificial electron donor, whereby the formation of hydrogen was also confirmed (see Figure 3). Reusability of the Au/TiO_2 catalyst after its use for 3 h was checked by filtering the catalyst and using it for a second run under the same conditions. Essentially the same kinetic profile shown in Figure 3 was obtained. Moreover, after two consecutive uses the filtered catalyst was characterized by chemical analysis and electron microscopy without observing changes with respect to those of the fresh catalyst. Chemical analyses of the solutions after the reaction

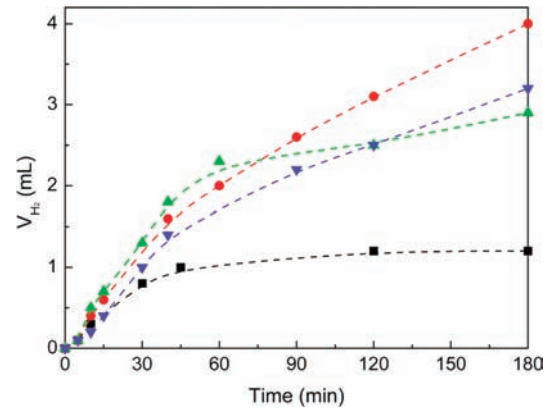

Figure 3. Volume of hydrogen evolved (V_{H2}) during the photocatalytic runs ($\lambda > 400$ nm) using catalysts with different gold loadings and methanol as sacrificial electrons donor: TiO_2 (■), Au(0.25%)/TiO_2 (●), Au(1.5%)/TiO_2 (▲) and Au(2.2%)/TiO_2 (▼).

Table 1. Initial Reaction Rate (r_0) and Amount of Hydrogen Evolved at 3 h of Irradiation ($V(H_{2,3h})$) for Visible Light Photocatalytic Runs Using Au/TiO_2 Catalysts with Different Gold Loadings

catalyst	$r_0 \times 10^2$ (mL min^{-1})	$V(H_{2,3h})$ (mL)
Au(0.25 wt %)/TiO_2	4.0	4.0
Au(1.5 wt %)/TiO_2	4.5	2.9
Au(2.2 wt %)/TiO_2	3.3	3.2

detected the presence of Au in a concentration that corresponds to 0.22% of the total Au content present in the fresh Au/TiO_2 (0.67 mg of Au in 45 mg of Au/TiO_2).

We also checked the influence of byproduct in the photocatalytic activity of Au/TiO_2. Using methanol as sacrificial electron donor, oxidized derivates, particularly formaldehyde and formic acid, are generated as byproducts, and it is of interest to determine how these two byproducts affect the photocatalytic activity of Au/TiO_2. Aimed at this purpose we carried out two additional experiments in where fresh Au/TiO_2 photocatalyst was irradiated in water−methanol solutions containing 0.1 M of these byproducts. The results show that the presence of formaldehyde plays a minor role in hydrogen evolution since an essentially similar temporal profile is shown in the absence or presence of formaldehyde. In contrast, it was observed that the presence of a 0.1 M concentration of formic acid increases significantly the rate of hydrogen evolution, probably due to the effect of acid pH on hydrogen evolution or the easier photocatalytic decomposition of formic acid to generate hydrogen.

Influence of Au Loading and Particle Size in Visible Light Photocatalytic Hydrogen Generation. In gold catalysis, it is well-known that gold loading is a very important parameter that determines the activity of the resulting material.[48] When changing the gold loading, several parameters such as gold particle size and morphology, TiO_2 surface coverage and population of residual hydroxy groups and metal dispersion are varied simultaneously. The balanced combination of all these factors determines that generally an optimal gold loading is observed for having the maximum catalyst efficiency. Typically, the most active materials in heterogeneous catalysis are those containing around 1 wt % gold loading. In the present case we prepared three samples of Au/TiO_2 using the standard deposition−precipitation method and compared their activities for visible light hydrogen generation with that of P25 TiO_2 devoid of any gold nanoparticles. The results are shown in Figure 3. As it can be seen there, we found a remarkable influence of gold loading in the range 0−2.2 wt % in agreement with many precedents in gold catalysis.[48] In our photocatalytic study two figures of merit, namely, the initial reaction rate (r_0) and the total hydrogen volume at final time (3 h), can be considered to assess the optimum catalyst performance. Table 1 lists both parameters for the series of Au/TiO_2 under study.

As it can be seen in Table 1, as well as in Figure 3, Au(0.25 wt %)/TiO_2 combines a high initial rate with high hydrogen productivity at 3 h, and it has the additional advantage of presenting a high gold economy. For this reason this loading was selected for additional studies. One point that deserves a comment is that at least one of the photocatalysts (Au(1.5 wt %)/TiO_2) exhibits fatigue during the hydrogen generation. This decrease in photocatalytic activity during the reaction is typically

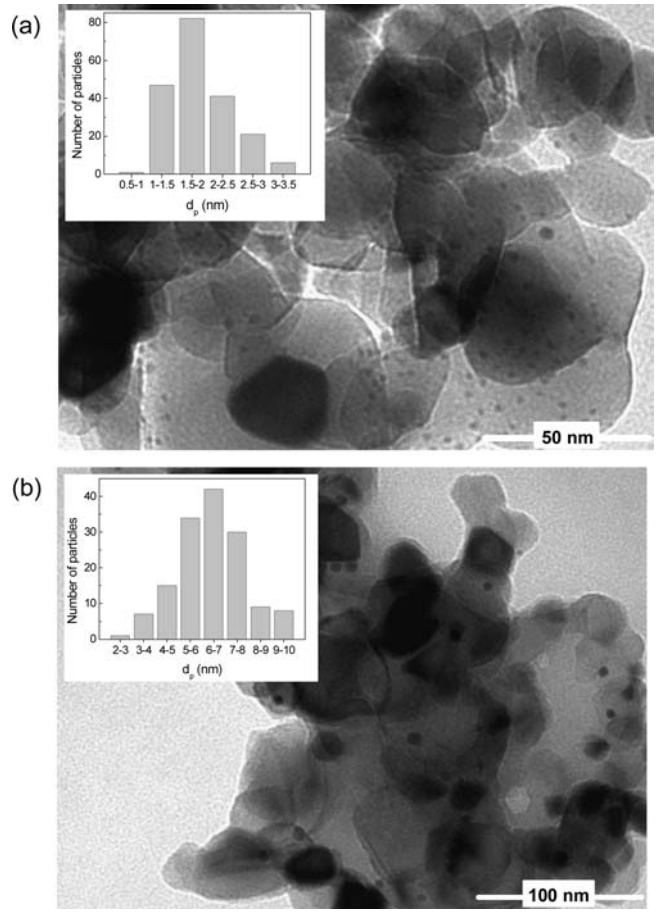

Figure 4. TEM micrographs and particle size distribution (insets) of Au/TiO_2 samples obtained at 200 °C and pH = 9.0 (a) and at 400 °C and pH = 4.5 (b).

due to deactivation probably caused by absorption of some byproduct (formic acid, formaldehyde, etc.) arising from the sacrificial agent decomposition during the course of the reaction. In any case the data presented showed that the materials exhibit a notable visible light activity that varies depending on the loading.

In gold catalysis, one important point is the preparation procedure, particularly calcination temperature as well as the gold particle size, shape and the plane of exposed gold crystallites. Haruta has previously reported that it is possible to control the gold particle size by careful control of the suspension pH value during the deposition process.[49] Based on this knowledge, we have prepared two sets of Au/TiO_2 samples, three of which were calcined at 200 °C and other three at 400 °C. In principle, higher calcination temperature causes the growth of the gold particle size but also the sintering between the gold and titania interphase. On the other hand, varying the pH value from 4.5 to 9.0 units allows gaining a certain control on the particle size distribution of gold. To illustrate the variation in the particle size distribution as a function of the calcination temperature and pH of the deposition step, Figure 4 shows representative TEM images of two of the Au/TiO_2 samples prepared as well as the corresponding statistical size distribution analysis showing the differences on the average gold particle size as a function of the preparation procedure. Unfortunately,

(46) Jakob, M.; Levanon, H.; Kamat, P. V. *Nano Lett.* **2003**, *3*, 353–358.
(47) Subramanian, V.; Wolf, E. E.; Kamat, P. V. *J. Am. Chem. Soc.* **2004**, *126*, 4943–4950.
(48) Corma, A.; Garcia, H. *Chem. Soc. Rev.* **2008**, *37*, 2096–2126.
(49) Tsubota, S.; Cunningham, D. A. H.; Bando, Y.; Haruta, M. *Stud. Surf. Sci. Catal.* **1995**, *91*, 227–235.

Table 2. Preparation Conditions (Deposition pH and Calcination Temperature), Average Gold Particle Size (d_p) and Wavelength for the Maximum Absorption of the Surface Plasmon Band (λ_{max}) for the Different Au/TiO_2 Samples

catalyst	pH	T_{calc} (°C)	d_p (nm)	λ_{max} (nm)
Au/TiO_2-1	4.5	200	4.91	550
Au/TiO_2-2	6.5	200	2.85	547
Au/TiO_2-3	9.0	200	1.87	552
Au/TiO_2-4	4.5	400	6.40	562
Au/TiO_2-5	6.5	400	4.20	560
Au/TiO_2-6	9.0	400	4.11	561

higher resolution and deeper analysis of the images will be necessary to determine if the photocatalytic process is sensitive to the morphology of the particles and, moreover, if the exposed Au crystal face also varies depending on the preparation procedure and deposition pH and if these parameters influence the photocatalytic activity.

Table 2 lists the codes of the Au/TiO_2 samples with indication of the preparation conditions and the average particle size. Importantly, it should be remarked that all the samples contained in Table 2 have a very similar gold loading around the optimum 0.25 wt % value previously determined.

As expected, due to the presence of gold nanoparticles, the UV−visible spectrum of the Au/TiO_2 samples exhibit in optical spectroscopy two bands: one in the visible region between 500 and 650 nm typical of the gold surface plasmon band, and another, stronger, with onset at 370 nm that is due to the bandgap transition of TiO_2 semiconductor (Figure 5).

Considering that our excitation light contains radiation of wavelength longer than 400 nm (see Figure 5) and also the influence of the presence of gold on the photocatalytic activity, we attribute this enhanced photocatalytic activity observed in Figures 2 and 3 to the contribution of gold nanoparticles as light harvesters and ability to inject electrons into the TiO_2 conduction band. Careful inspection of the position of the surface plasmon band reveals that the samples calcined at 200 °C exhibit very similar wavelength maxima around 550 nm that is different and blue-shifted from the other set of samples calcined at 400 °C where the wavelength maxima of the gold surface plasmon band appears around 561 nm. The actual wavelength maximum for each sample is also given in Table 2. With this set of samples, photocatalytic hydrogen generation using methanol as sacrificial electron donor and visible light

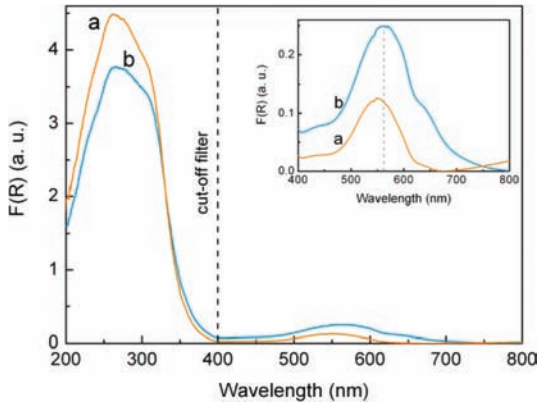

Figure 5. UV−vis spectra of the Au/TiO_2-1 (a) and Au/TiO_2-6 (b) photocatalysts plotted as the Kubelka−Munk function of the reflectance (R). The inset shows an expansion of the gold surface plasmon band. The dashed vertical line indicates the cutoff wavelength of the filter used in the photocatalytic experiments.

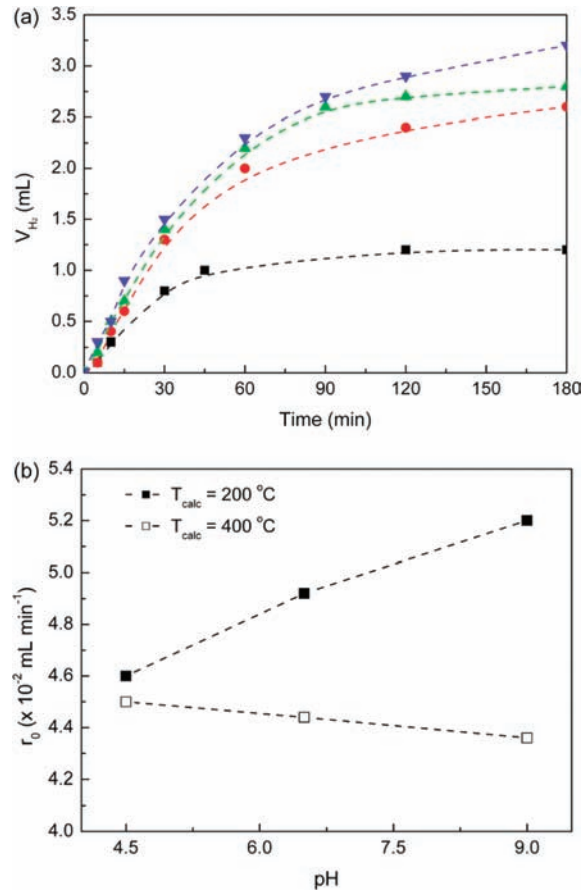

Figure 6. (a) Volume of hydrogen evolved (V_{H2}) during the photocatalytic runs using methanol/water (3/1 v/v) in the presence of catalysts obtained at 200 °C and different pH: TiO_2 (■), Au/TiO_2-1 (●), Au/TiO_2-2 (▲) and Au/TiO_2-3 (▼). (b) Initial reaction rates (r_0) obtained for the catalysts synthesized at different calcination temperature and pH.

was carried out. Figure 6a shows the temporal evolution of hydrogen formation as a function of the irradiation time and the catalyst present.

Concerning the initial reaction rate (Figure 6b) some trends were observed. Those samples calcined at lower temperature exhibited higher activity than those calcined at 400 °C. Also for the most active samples (200 °C calcination temperature), the initial reaction rate of hydrogen formation increases as the gold particle size decreases. Therefore, based on this it can be concluded that the intrinsically more efficient samples of Au/TiO_2 should contain the optimum gold loading with the smallest particle size. However, we notice that for the series of Au/TiO_2 calcined at 400 °C the trend of the pH deposition on the photocatalytic activity is opposite (see Figure 6b). Therefore, it appears that other factors besides the particle size are coming into play.

The previous discussion on the photocatalytic activity is based on the initial reaction rate that reports on the intrinsic photocatalytic activity of fresh samples. However, as commented earlier when observing deactivation of some photocatalysts, long-term hydrogen productivity depends not only on the intrinsic activity but also on the catalytic stability and deactivation processes. Thus, it is frequently observed in catalysis that the most active material becomes rapidly deactivated and the long-term performance is worse than that of other materials exhibiting a good balance between initial activity and long-term stability. This is apparently the case here since those

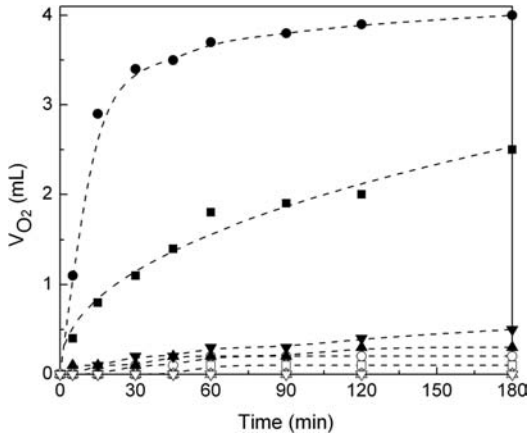

Figure 7. Volume of oxygen (V_{O2}) evolved during the photocatalytic runs using Au(1.5 wt %)/TiO_2 and P25 TiO_2 under UV and visible light (λ > 400 nm) using either $AgNO_3$ or $(NH_4)_2Ce(NO_3)_6$ as sacrificial electron acceptors. ●: Au/TiO_2, UV, $(NH_4)_2Ce(NO_3)_6$. ■: Au/TiO_2, UV, $AgNO_3$. ▼: Au/TiO_2, vis, $(NH_4)_2Ce(NO_3)_6$. ▲: Au/TiO_2, vis, $AgNO_3$. O: TiO_2, UV, $(NH_4)_2Ce(NO_3)_6$. □: TiO_2, UV, $AgNO_3$. Δ: TiO_2, vis, $AgNO_3$. ▽: TiO_2, vis, $(NH_4)_2Ce(NO_3)_6$.

samples calcined at 400 °C exhibit better stability during operation of the photocatalytic hydrogen generation. This is not surprising since higher calcination temperatures increase catalytic stability by promoting the grafting and the interfacial contact between gold and the support. Therefore, concerning the total H_2 production at 3 h irradiation time, the differences observed based on the initial reaction rate disappear and the performance of the samples calcined at 400 °C becomes similar to the performance of those prepared at 200 °C.

UV and Visible Light Photocatalytic Oxygen Evolution Using Au/TiO_2. Once the study of the reduction semireaction was complete, we used the same set of samples and the same excitation source to determine the possibility of photocatalytic oxygen generation. Oxygen generation from water requires much higher oxidation potential than the reduction potential needed for hydrogen evolution. In addition to the thermodynamic requirement of holes having higher oxidation potential than 1.26 V, oxygen evolution is considered mechanistically a complex process since the formation of one oxygen molecule involves four electrons and the creation of oxygen−oxygen bonds absent in the water molecule. For the mechanistic complexity, oxygen generation is considered frequently the bottleneck for the overall water splitting.[50,51]

The samples under study containing gold nanoparticles were found also to exhibit photocatalytic activity for O_2 generation from water under both UV and visible light excitation. Figure 7 shows a temporal profile of O_2 evolution for Au(1.5 wt %)/TiO_2 and P25 TiO_2 under UV and visible light (λ > 400 nm) excitation using either $AgNO_3$ or $(NH_4)_2Ce(NO_3)_6$ as sacrificial electron acceptors.

As can be seen in Figure 7, $(NH_4)_2Ce(NO_3)_6$ as sacrificial electron acceptor promotes higher oxygen evolution than $Ag(NO_3)$, probably because in the latter case the formation of black silver particles or formation of core/shell Au/Ag particles reduces the efficiency of the photocatalytic oxygen evolution. Recently it has been observed that core/shell Au/Ag nanoparticles can be formed upon photolysis of Au nanoparticles in the presence of Ag salts, and a similar process can occur here.[52−55] If this were the case, then the photocatalytic activity would decrease due to the coverage of Au nanoparticles by a shell of Ag.

Scheme 3. Proposed Rationalization of the Photocatalytic Activity of Au/TiO_2 Forming O_2 upon Excitation of the Gold Surface Plasmon Band

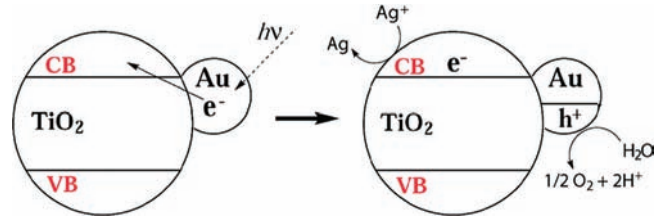

Firm experimental evidence of oxygen evolution upon excitation at the gold surface plasmon band was again obtained by using as excitation light a monochromatic laser operating at 532 nm. The results show that no oxygen is evolved performing the experiment using P25 TiO_2, while in contrast the presence of Au nanoparticles in Au(1.5 wt %)/TiO_2 introduces visible light photoactivity. According to Scheme 3, the positive holes located on Au nanoparticles should have an oxidation potential higher than 1.26 V.

Typically metals are devoid of any oxidation activity. However, when the particle size is reduced a transition between the band theory predicts a change from the characteristic bands of bulk metals to discrete atomic orbitals present in atoms occurring in the nanometric scale. Small Au clusters (below 2 nm) can exhibit frontier HOMO/LUMO orbitals, and electron holes in the HOMO orbital can have higher oxidation potential than larger nanoparticles. The situation is, however, complex since variation of the HOMO/LUMO orbital energy and the presence of separate valence and conduction bands will influence also the absorption of light and intensity of the corresponding surface plasmon band associated with the nanoparticles. Thus, very likely small nanoparticles having discrete energy levels are those that do not have intense visible light absorption.

Attempts to obtain electrochemical evidence of the oxidation potential of Au(1.5 wt %)/TiO_2 allowed detection of some reversible oxidation peaks at −1.14 V semipotential in films of this material supported on conductive ITO electrode (Figure 8). These peaks could be attributable to the electrochemical generation of holes on Au nanoparticles since analogous measurements with P25 TiO_2 (pH of zero point charge about 6.0) do not allowed detection of any peak in the available oxidation window. Although further studies are necessary to firmly assign the electrochemical peaks observed for Au(1.5 wt %)/TiO_2 to the positive holes generated in photocatalysis, the presence of electrochemical response Au(1.5 wt %)/TiO_2 is compatible with the observed photocatalytic oxygen evolution.

We noticed however that the oxidation power of the electrochemical oxidation peak at the maximum of the current intensity (−1.14 V) is lower than the thermodynamic oxidation potential required to generate oxygen from water (1.26 V). In

(50) Kanan, M. W.; Nocera, D. G. *Science* **2008**, *321*, 1072–1075.
(51) Kanan, M. W.; Surendranath, Y.; Nocera, D. G. *Chem. Soc. Rev.* **2009**, *38*, 109–114.
(52) Gonzalez, C. M.; Liu, Y.; Scaiano, J. C. *J. Phys. Chem. C* **2009**, *113*, 11861–11867.
(53) Marin, M. L.; McGilvray, K. L.; Scaiano, J. C. *J. Am. Chem. Soc.* **2008**, *130*, 16572–16584.
(54) McGilvray, K. L.; Decan, M. R.; Wang, D. S.; Scaiano, J. C. *J. Am. Chem. Soc.* **2006**, *128*, 15980–15981.
(55) Scaiano, J. C.; Billone, P.; Gonzalez, C. M.; Maretti, L.; Marin, M. L.; McGilvray, K. L.; Yuan, N. *Pure Appl. Chem.* **2009**, *81*, 635–647.

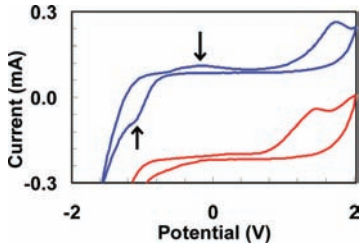

Figure 8. Cyclic voltammetry of a film of Au(1.5 wt %)/TiO_2 supported on a FTO electrode immersed in electrolyte. The bottom voltammogram corresponds to the response of TiO_2 film on ITO electrode recorded under identical conditions. The arrows point to the specific peaks observed for Au(1.5 wt %)/TiO_2 during the reduction (pointing up) and the oxidation (pointing down) scan.

Table 3. Initial Reaction Rate (r_0) and Amount of Oxygen Evolved at 3 h of Irradiation for Photocatalytic Runs Using Au/TiO_2 Catalysts Obtained at Different Calcination Temperature and pH[a]

catalyst	$r_0 \times 10^2$ (mL min^{-1})	$V(O_{2,3h})$ (mL)
Au/TiO_2-1	2.4	1.2
Au/TiO_2-2	3.0	1.3
Au/TiO_2-3	3.2	1.4
Au/TiO_2-4	2.3	1.2
Au/TiO_2-5	2.2	1.1
Au/TiO_2-6	2.2	1.0
TiO_2		<0.1

[a] See Table 2 for conditions.

this regard it has to be commented that cyclic voltammetry shows broad peaks, probably reflecting a distribution of Au nanoparticles with different oxidation potentials, depending on the particle size. It could be that not all the particles could be able to oxidize water generating oxygen, but only the fraction of the gold nanoparticles in where the oxidation potential fulfills the thermodynamic requirements, i.e. those with oxidation potential higher than 1.26 V. The others, even if they are photochemically excited, will not have enough oxidation capacity to generate oxygen.

In general agreement with the previous findings for the photocatalytic hydrogen generation, we also observed that the initial reaction rates and the final oxygen volume at 3 h depend on the gold particle size and calcination temperature. We have observed for oxygen the same trend as for hydrogen, the most active Au(0.25 wt %)/TiO_2 photocatalyst for oxygen generation being the same as for hydrogen generation, i.e., the Au/TiO_2 material prepared at pH 9.0 and calcined at 200 °C (Au/TiO_2-3), with a gold average particle size of 1.87 nm (Table 3).

Quantum Yields for Visible Light Hydrogen and Oxygen Generation. The most important finding of our study is the visible light photocatalytic activity for water splitting of Au/TiO_2. We determined the quantum yield for the independent hydrogen and oxygen semireactions using sacrificial reagents for the most efficient Au/TiO_2-3 sample using monochromatic light. In order to ensure the selective excitation of gold surface plasmon band we selected for the quantum yield measurements 560 nm that is close to the λ_{max} for gold nanoparticles and far from the onset of the TiO_2. For comparison we have attempted to measure the quantum yield of hydrogen and oxygen generation for TiO_2 at the same excitation wavelength. The results obtained (Table 4) prove quantitatively the photocatalytic activity for water splitting of titania as a consequence of the presence of gold nanoparticles. In this context Domen and coworkers have reported $(Ga_{1-x}Zn_x)(N_{1-x}O_x)$ photocatalysts as one of the most efficient materials for water splitting, having an efficiency of 2−3%.[56] Therefore, our Au/TiO_2 absorbing at long wavelengths exhibits an activity that is not far from that of other visible light water splitting photocatalysts.

Table 4. Quantum Yield (Φ) of Hydrogen and Oxygen Generation Determined by Ferrioxalate Actinometry at 560 nm

catalyst	Φ_{H2} (%)	Φ_{O2} (%)
TiO_2	<0.1	<0.1
Au-TiO_2-3	7.5	5.0

The low quantum yield values for TiO_2 are compatible with the negligible absorption of TiO_2 at this long wavelength. In any case, the data of Table 4 clearly show that the light harvesting component is gold nanoparticles at least for long wavelengths.

Conclusions

In the present work, by using a monochromatic 532 nm laser excitation and a UV cutoff filter ($\lambda > 400$ nm) that ensures that the light is absorbed exclusively by gold nanoparticles in combination with the quantum yield measurements we have demonstrated that gold can have an additional role as light harvester besides gas evolution center. We have found that, using excitation wavelengths corresponding to gold plasmon band, gold nanoparticles absorb photons and inject electrons into the semiconductor conduction band (Schemes 2 and 3). This photoinduced electron injection into the conduction band of a semiconductor is unusual for a metal, but the nanometric size of the gold particles and the operation of quantum size effects should be responsible for the occurrence of this mechanism. Electrons in the titania conduction band and holes in certain gold nanoparticles have adequate potential to generate hydrogen and oxygen from water, respectively. We have also found that the gold particle size and calcination temperature play a certain role, influencing the catalytic activity. Apparently the combination of appropriate loading, small particle size and the presence of surface hydroxyl groups (low calcination temperatures) favors the photocatalytic activity of the materials.

Acknowledgment. Financial support by the Spanish Ministry of Science and Innovation (CTQ 2009-11586 and Consolider Ingenio 2010, CSD2009-0050, MULTICAT) is gratefully acknowledged. Cláudia G. Silva thanks Fundação para a Ciência e a Tecnologia (Portugal) for the post-doctoral fellowship (SFRH/BPD/48777/2008). Dedicated to Prof. Rafael Suau in memorian.

JA1086358

(56) Maeda, K.; Domen, K. *Chem. Mater.* **2010**, *22*, 612–623.